Reduced inorganic sulfur in surface sediment and its impact on benthic environments in offshore areas of NE China

Yanqing Sheng[1, *], Qiyao Sun[1], Simon Bottrell[2], Robert Mortimer[3]

[1] Research Center for Coastal Environmental Engineering Technology of Shandong Province, Yantai Institute of Coastal Zone Research, Chinese Academy of Sciences, Yantai 264003, P.R. China

[2] School of Earth and Environment, University of Leeds, Leeds LS2 9JT, UK

[3] School of Animal, Rural and Environmental Sciences, Nottingham Trent University, Brackenhurst campus, Southwell, Nottinghamshire, NG25 0QF, UK

Abstract

Geochemical cycling and biological toxicity of sulfur in marine sediments is closely related to the activity of organisms. This study investigated the distribution and potential impact on benthic environments of acid volatile sulfur (AVS), chromium (II)-reducible sulfur (CRS), elemental sulfur (ES), total S, C, N and Fe in superficial sediments across the Bohai Sea, Yellow Sea and East China Sea. The composition of reduced inorganic sulfur in the three study areas was dominated by CRS (averaging 72% of total reduced inorganic sulfur). The low AVS content

[*] Corresponding author: Tel.: +86 535 2109265; Fax: +86 535 2109000; E-mail address: yqsheng@yic.ac.cn

(average of 1.12 µmol g^{-1}) of the sediments and the low values of AVS/CRS (average 0.34 µmol g^{-1}), degree of pyritization and degree of sulphidization indicate that there is sufficient available iron in the sediment to restrict the threat of sulphide toxicity to benthic organisms in most of the study areas. However, high organic matter loads in parts of the study areas have resulted in enhanced accumulation of AVS, resulting in a higher toxicity risk.

Keywords: Sulfur compounds; Sedimentary environments; Offshore; Benthic environment

1. Introduction

Sulfur is essential to life and one of the key players in global biogeochemical cycles. However the most reduced form, sulfide, is generally toxic to organisms and influences water quality (Bagarinao, 1992; Sheng et al., 2011). Sulfur is cycled between and fixed in many different forms in marine sediments (Morse and Berner, 1995; Canfield et al., 2005; Bottrell et al., 2009; Alvarez and Rubio, 2012). Therefore, understanding sulfur speciation in marine sediments is essential in evaluating its response to environmental change and the potential biological impact of sulfide. The availability of sulfide in the coastal environment will have implications for overlying water quality.

The sulfur cycle in marine sediments can be divided into reductive and oxidative processes. The reductive side of the cycle is driven by microorganisms that reduce

sulfate to sulfide in anaerobic environments and rates of sulfate reduction can be very high under such conditions (Morse et al., 2007; Tarpgaard et al., 2011).

$$SO_4^{2-} + 2CH_2O \Rightarrow H_2S + 2HCO_3^- \quad (1)$$

In the oxidative side of the cycle sulfide reacts with a variety of oxidants such as O_2 and Fe(III) oxides to produce sulfate or intermediate S forms (e.g. elemental S). The majority of the sulfide produced in marine sediment is reoxidized (Canfield and Thamdrup 1994; Poulton 2003; Bottrell and Newton, 2006). Sulfide produced is also removed by reaction with mineral-derived Fe, initially producing a monosulfide "FeS" which transforms to more stable pyrite, FeS_2 (Berner 1970, 1984). However, the reactivity of mineral iron forms is highly variable (Canfield et al. 1992) and may limit the removal of sulfide. Where supply of oxidants is also restricted, production of sulfide may outcompete rates of removal and concentrations of toxic sulfide will increase in shallow pore-waters and bottom waters (Phillips et al. 1997). Furthermore, iron monosulfide species formed in sediment are often highly reactive and will rapidly react with and remove dissolved oxygen from bottom waters if sediment is resuspended.

The reactivity of sulfide stored in sediment when resuspension occurs is dependent on the form in which sulfide is present; dissolved sulfide is most reactive, followed by monosulfide, and pyrite is least reactive (Morse and Rickard 2004). In many sediments conversion of monosulfide to pyrite is rapid (Schoonen and Barnes 1991; Butler and Rickard 2005) such as reoxidation of AVS in the uppermost layer

and thus monosulfide concentrations are low or negligible (e.g. Rozan et al. 2002; Rickard and Morse 2005). However in other situations (e.g. high pH (>7.8) sediments and under organic-rich eutrophic conditions) Fe monosulfides are persistent and represent a significant pool of reactive sulfide in the sediment (Hurtgen et al. 1999; Morse 1999; Burton et al. 2011; Morgan et al., 2012). Sulfide is toxic to aquatic plants and organisms. Its accumulation in upper sediment layers in coastal areas exerts an impact upon not only local benthos but also the pelagic biota due to the potential release of free sulfide into the water column (Bagarinao, 1992). Furthermore, re-suspension of sediment can result in oxidation of H_2S and reactive sulfides, changing the redox conditions of the overlying water and leading to hypoxia at the sea floor (Phillips et al., 1997; Sorokin and Zakuskina, 2012). Oxidation of monosulfide in surface sediments may also lead to the release of toxic heavy metals (coprecipitated with FeS) into more bioavailable forms, such as dissolved Cu and Zn (Simpson et al., 2012; Rodrigues et al., 2013). Most organisms live within oxic surface sediments or in oxygenated microenvironments created within sub-oxic and anoxic sediments (Simpson et al., 2012), and hence are vulnerable to shifts in redox and associated changes in sulfur speciation and toxicity.

The degree of pyritization (DOP) and the degree of sulphidization (DOS) are two parameters that can be used to distinguish between situations where pyrite and Fe sulfide formation is either C- or Fe-limited and to measure the completeness of the reaction of reactive Fe (operationally defined as the fraction of Fe that is soluble in 1 M HCl for 16h) with aqueous sulfide (Raiswell and Berner, 1985). In sediments that

contain a significant amount of Fe monosulfide, DOP underestimates the amount of Fe that has reacted with H_2S (Boesen and Postma, 1988). Instead, DOS represents the degree to which reactive Fe has been transformed into sulfide and, therefore, provides a better indication of Fe limiting conditions (Yin et al., 2008). In sediments where Fe availability becomes limiting pore-water sulfide concentrations are likely to increase, enhancing the likelihood of sulfide toxicity. Conversely, if sulfide production is limited by the availability of a labile organic substrate, pore-water sulfide concentrations may be very low.

The Bohai Sea, Yellow Sea and East China Sea are situated north-east (NE) of China. They are important production bases for fishery and marine industries. This study area can be characterized as a region surrounded by areas of high population growth and economic development. A large amount of pollutants are discharged into these areas in industrial and municipal wastewaters via rivers (i.e. Yellow River, Yangtze River and other smaller rivers), along with excess inputs of nutrients from mariculture. This pollution may influence the cycles of iron, sulfur and phosphorus (Rozan et al., 2002), leading to offshore eutrophication and benthic macroalgal blooms, especially large offshore phytoplankton blooms e.g. *enteromotpha prolifera* in Yellow Sea (Liu et al., 2013). Previous studies on the effects of biogenic elements in sediments in these areas were focused mainly on carbon, nitrogen and phosphorus (Liu et al., 2004; Liu and Yin, 2007). However, to date, only limited effort has been devoted to the study of sedimentary geochemistry of reduced inorganic sulfur (RIS) in the offshore areas of NE China (Kang et al., 2014), and its potential impact on the

marine ecosystem remains unclear.

In this study, acid volatile sulfur (AVS), chromium (II)-reducible sulfur (CRS, pyritic sulfur), elemental sulfur (ES), total sulfur (TS), reactive iron, total organic carbon (TOC) and total nitrogen (TN) were analyzed in surface sediments from the study area. The partitioning of RIS was used to understand sulfur biogeochemistry within the sediments, and to predict the potential for ecotoxicological risk due to release of toxic sulfide.

2. Methods and materials

2.1 Samples collection and handling

A total of 82 sediment samples were collected from the Bohai Sea, Yellow Sea and East China Sea (Fig. 1). Surface sediments (0-20 cm) were collected using a stainless steel grab sampler and were immediately isolated from the atmosphere in plastic zip-lock bags with all air expelled by N_2 gas (a N_2 gas cylinder was aboard ship). Samples were frozen and stored in an icebox (-20°C) until arrival at the laboratory. Samples were processed immediately upon return to the laboratory. In the laboratory, the plastic sample bags were first flushed with high purity N_2 again. Samples were then homogenized under this inert atmosphere (a glove box) by mixing with a plastic spatula. Four replicates were used throughout.

Fig. 1

2.2 Sample analysis

The reagents used were all analytical grade or above, and deionized water (milli-Q) was used to prepare reagent solutions. All glass and plastic were soaked in 10% HNO_3 for 48 h and rinsed with milli-Q water three times before use. Total organic carbon (TOC) in sediments was determined by a Shimadzu TOC-V_{CPH}/SSM-5000A. Total nitrogen (TN) and total sulfur (TS) were determined by an Elementar vario MACRO cube CHNS analyzer. The precision of the measurements was within 5% based on three replicate sediment analyses. Prior to grain size analysis, each sediment sample was treated with sodium hypochlorite (NaOCl) to remove organic matter. Sample granulometry was analyzed using a Malvern Mastersizer 2000 laser diffractometer capable of analyzing particle sizes between 0.02 and 2,000 μm. The percentages of samples in each of the following three grain-size groups were determined: < 4 μm (clay), 4-63 μm (silt), and >63 μm (sand).

The separation and determination of AVS, CRS and ES were conducted using a modified procedure described by Newton et al. (1995) and Hsieh & Shieh (1997). Reagents and extraction steps of sulfur species separation are the same as the description of Hsieh & Shieh (1997), the detection of H_2S is the same as the description of Newton et al. (1995). In this method, a thin glass pipe (with N_2 gas inside) was dipped into corresponding solutions (shaking occasionally) to accelerate the emission of H_2S (1.5 h). All subsequent processing of sediment was performed under a N_2 atmosphere inside a glove box at room temperature. Briefly, AVS, CRS

and ES were separated sequentially by 6 M HCl, acidic Cr (II) and Cr (II) plus N, N-dimethylformamide, respectively, using pure N_2 as carrier gas to purge and trap H_2S, at a temperature of ~ 60 °C (by electric hot plate). The liberated H_2S was trapped in a 0.1 mol L^{-1} $CuCl_2$ solution. The amount of H_2S evolved from the sample for each solid-phase RIS species was determined by titrating the Cu remaining in solution with 0.1 mol L^{-1} EDTA (assuming a precipitate of CuS stoichiometry). Three to four drops of glycine cresol red (0.5% aqueous) was used as an indicator and the titration was buffered with 70 ml of 1 mol L^{-1} sodium acetate solution (adjusted to pH 5.5 with acetic acid). The endpoint was sharp and marked by a colour change from dark blue to a light green. Sulfide solutions (Na_2S) with concentrations of 0.5 and 1 mg L^{-1} were used in recovery experiments. Average sulfide recovery rate was 96%. Measured sulfide data were converted to real sulfide contents after correction for the recovery rate. The precision of triplicate analysis was within 5% for different fractions of RIS. The fractions of Fe were determined by sequential acid digestion. Reactive Fe is the fraction of Fe that is soluble in 1 mol L^{-1} HCl (16h, Fe_R) and pyrite Fe (Fe_{py}) is the Fe that is soluble in concentrated HNO_3, after removal of the Fe associated with silicates and organic matter (Huerta-Dı′az & Morse, 1990). The concentrations of different Fe fractions (extracted by corresponding acid) were detected by an Atomic Absorption Spectrometer (TAS 990, Beijing Purkinje General Instrument Co.Ltd., Beijing), precision was to within 2% based on triplicate analysis.

2.3 Data calculation

DOP was taken to be the percentage of pyrite-Fe in the bioavailable iron, which was calculated as $Fe_{py}/(Fe_R + Fe_{py})$ (Berner, 1970). Fe_{py} was calculated from FeS_2 stoichiometry. DOS was taken to be the percentage of Fe that has been transformed into sulfide, which was defined by $(Fe_{py} + Fe_{AVS})/(Fe_{py} + Fe_R)$ (Boesen and Postma,1988). Fe_{AVS} is sulfide-bound Fe(II) assuming that AVS predominantly occurs as FeS, though this assumption remains controversial (Morse and Rickard, 2004; Rickard and Morse, 2005).

3. Results and discussion

3.1 Distribution of grain size

Fig. 2

The grain size of the sediments plays a significant role in the accumulation of organic matter, and can influence the spatial distribution of C, N and S (Zhou et al., 2007). The variations of grain size in the surface sediments are shown in Fig. 2. The data reveal a predominance of silt (4-63 μm), which accounted for an average of 57%, 57% and 47% of the particles in Bohai Sea, Yellow Sea and East China Sea, respectively. Compared to the East China Sea, high proportions of silt in the Bohai Sea and the Yellow Sea are most likely related to transport of suspended sediments down the Yellow River (Qiao et al., 2010). The surface sediments of Bohai Sea were dominated by silt, except for samples B52, B53 and B54 (Fig. 1). These sites were

located in the main water exchange channel between the Bohai Sea and the Yellow Sea (Liu et al., 2004), so the small particles (clay) may be winnowed by strong water currents, resulting in a predominance of sand in this area (Fig.2). In the East China Sea, driven by the Zhejiang-Fujian coastal current, a large amount of fine grained particulates from the Yangtze Estuary are transported southward along the coast and trapped in the inner shelf by the blocking of the northward warm Taiwan current offshore, developing mud wedges outside the Yangtze River mouth (Xu et al., 2009). Therefore, at site E01 (Fig. 1), the sediment was dominated by fine grained particulates, with silt and clay accounting for ~ 97% of total grains (Fig. 2).

3.2 Distribution of TOC, TN and TS

The surface sediments were characterized by variable concentrations of TN, TOC and TS. TN varied from 0.03-0.21% (% dry weight of the sediment), TOC from 0.11- 2.49% and TS from 0.11-0.40%. The average TN in the Bohai Sea, Yellow Sea and East China Sea were 0.07%, 0.08% and 0.06%, respectively. The averages for TOC were 1.23%, 1.07% and 1.09% respectively (Fig. 3). The highest TOC contents were recorded at site B66 (2.3%) in the Bohai Sea, B31 (2.5%) in the Yellow Sea and E01 (1.6%) in the East China Sea. In the Bohai Sea, TN, TOC and TS exhibited high values in Bohai Bay and Laizhou Bay. In the Yellow Sea, the TOC and TS contents in sediments at B31 and B32 were high (2.5% and 1.5% respectively), indicating high organic pollution loads in these areas, most likely related to the Dalian crude oil spill in 2010 (Lv et al., 2011). This organic pollution may provide an additional substrate

for sulfate reduction and lead to increased sulfide production and accumulation in the sediment.

Fig. 3

3.3 Distribution characteristics of different fractions of RIS

Fig. 4 presents the AVS, CRS and ES concentrations in the surface sediment samples of the Bohai Sea, Yellow Sea and East China Sea. The AVS, CRS, and ES values were in the ranges 0.2-4.1μmol g^{-1}, 0.6-101μmol g^{-1}, and 0.5-3.9μmol g^{-1}, respectively. AVS contents in the Bohai Sea, Yellow Sea and East China Sea are close to the ranges of AVS contents for Jiaozhou Bay sediments (0.06-13.7μmol g^{-1}) (Zhu et al., 2012) and East China Sea shelf sediments (0-25μmol g^{-1}) (Lin et al., 2000; Zhu et al., 2013). For CRS, the concentrations are 0.6-101μmol g^{-1}, dominating the total RIS in all studied areas, with an average 75% share in the Bohai Sea, 59% in the Yellow Sea and 87% in the East China Sea (Fig. 4 and Table 1). This finding was consistent with the reports of Zhu et al. (2012) in Jiaozhou Bay (CRS: 8.7-51.1μmol g^{-1}), Sheng et al. (2013) in the coastal zone of the Yellow Sea (CRS: 5.5-13.1μmol g^{-1}) and Zhu et al. (2013) in the East China Sea inner shelf (CRS: 2.7-38.3μmol g^{-1}). In this study, although there are some values of RIS at sites B30, B31 and B32 associated with an oil spill, even these highest values (101.2 μmol g^{-1}) are much lower than the peak value for the southern East China Sea slope sediments (range: 0-240 μmol g^{-1}) (Lin et al., 2002). CRS dominates over AVS in the RIS pool in the Bohai Sea, Yellow

Sea and East China Sea sediments and thus in all these locations AVS produced by sulfate reduction has been efficiently transformed to pyrite and there is limited accumulation of reactive monosulfide. Because of high concentrations of reactive iron (average is approximately 100 μmol g^{-1}) in these areas, the sulfide may be removed quickly by the formation of FeS, then it was transformed to FeS_2 due to sufficient ES (0.5-3.9 μmol g^{-1}) is present under anoxic conditions (reoxidation of AVS would be restrained because of limited free oxygen in benthic bottom), resulting in high concentration of CRS. Overall, accumulation concentrations of labile sulfides (i.e. AVS) in the study area is much lower than levels known to be potentially toxic for aquatic biota (200 mg S L^{-1} of wet silt, Sorokin and Zakuskina, 2012), suggesting the environmental conditions are low risk for the local marine ecosystem.

Generally, RIS concentrations were higher in the Yellow Sea than in the Bohai Sea and East China Sea, especially at sites B30, B31 and B32. This phenomenon is consistent with the variation of TOC and TS in same sites, and is most likely related to the Dalian crude oil spill summer 2010 (Lv et al., 2011). Deposited crude oil may result in a high load of organic pollutants in these areas, increasing TOC accumulation in the sediment (B30, B31 and B32). Furthermore, these organic compounds may provide an additional substrate for sulfate reduction and lead to increased sulfide production and accumulation in the sediment. Whilst the oil spill has modified the sediment geochemistry and increased AVS content, in the samples analyzed this increase is small and lies within the range of many sediments that have not been polluted by oil spills.

Fig. 4

3.4 Relationships between C, N, S and different fractions of RIS

The atomic molar ratios of C/N, C/S and AVS/CRS are listed in Table 1. C/N and C/S are ratios of TOC concentrations against TN and TS concentrations, respectively. C/N is widely applied in biogeochemical studies of terrestrial, riverine, estuarine, and marine environments, most commonly to estimate the fraction of terrestrially derived organic matter in marine sedimentary samples (Meyers, 1997). In this study, the C/N ratio (molar ratio) varied from 10.1 to 48.4 (average: 18.9) in the Bohai Sea, 7.7-41.3 (average: 15.1) in the Yellow Sea and 16.5-20.7 (average: 17.8) in the East China Sea (Table 1). These results suggest that the studied areas are abundant in terrestrial-derived organic matter with high C/N ratios (always higher than 10) (Meyers, 1997), associated with material rich in cellulose which originates from terrestrial vascular plants and reaches the sediments via rivers, i.e. Yellow River and Yangtze River.

TS and TOC/TS (C/S) are used for studying oxic/anoxic conditions in marine environments (Berner, 1984). The C/S ratios varied from 6.1 to 37.5, with an average of 12.8 in the Bohai Sea, 1.3-24.2 (average: 10.3) in the Yellow Sea and 6.5-17.0 (average: 10.3) in the East China Sea. Generally, the ratio of C/S in normal marine sediment (deposited under an oxic water column) is 2.0-3.8 (Berner, 1982). Overall, the C/S ratio in this study was highly variable at 1.3-37.5 (average: 11.4), with values

in most sampling sites higher than is normal for marine sediments. This can be explained by the impact of freshwater input and mariculture activity, which can both significantly influence C/S ratios, e.g. site B66 (37.5), is close to the Yellow River estuary (with high TOC and low RIS values in sediment); site H1 (24.3) is close to Qingdao city, where there are many large wastewater treatment plants (over 1 million tons discharged per day); site H35 (21.7) is in a mariculture area. Generally, sewage and mariculture contribute more C but not more S, resulting in high C/S ratios. The result indicates that sulfate reduction or RIS accumulation was variable in surface sediment of different areas, and may be influenced by anthropogenetic activities (organic matter input) and redox conditions. AVS/CRS varied from 0.14 to 1.22, with an average of 0.48 in Bohai Sea, 0.01-1.09 (average: 0.22) in Yellow Sea and 0.02-0.11 (average: 0.06) in East China Sea. Low ratios indicate that the sediment in these areas poses a low threat of toxicity to benthic organisms because CRS is more stable and less likely to release sulfide or metals than AVS, which is more soluble and reactive.

3.5 DOP and DOS

The relationship between sulfide and iron plays an important role in controlling of the sulfur cycle. As shown in Table 1, both DOP and DOS for the three areas are generally close to each other, with DOP ranging from 0.01 to 0.31 (averages of 0,02 for the Bohai Sea, and 0.04 for both the Yellow Sea and East China Sea) and DOS ranging from 0.02 to 0.33 (averages of 0.04 for the Bohai Sea, 0.05) for the Yellow

Sea and 0.04 for the East China Sea. DOS values are slightly higher than the DOP values, which perhaps reflects the reaction of FeS and H_2S to form pyrite (Rozan et al., 2002). The three areas have much lower DOP and DOS in comparison with the averages for estuarine and bay sediments of the Gulf of Mexico (DOP 0.56-0.95 and DOS 0.63-2.66) (Morse et al., 2007), but are consistent with DOP (0.05-0.25) and DOS (0.05-0.39) for Jiaozhou Bay sediment in the Yellow Sea (Zhu et al., 2012). On the basis of the simple comparison above, it is inferred that maybe there was low availability of labile organic matter in the study areas, which has been limiting sulfide production (Zhu et al., 2012), resulting in low values of DOP and DOS. Furthermore, high concentrations of reactive iron (average is approximately 100 μmol g^{-1}) and low values of DOP and DOS found in the present study further indicate that pyritization and sulfidization are not being limited by the availability of reactive Fe. Thus in these sediments the supply of mineral-Fe has been amply sufficient to match net sulfide production and thus limit the sulfide toxicity hazard.

Table 1

4. Conclusions

In order to elucidate the geochemical processes controlling the formation and stability of RIS species and its bioavailability in surface sediments, we have examined the relationship between the spatial variations in the values of sedimentary grain size, TOC, TN, TS, AVS, CRS, ES, C/N ratio, C/S ratio, AVS/CRS ratio, DOP and DOS in

Bohai Sea, Yellow Sea and East China Sea. In the study area, CRS was the dominant fraction of RIS, indicating the RIS is dominantly in a stable form and thus poses a low threat of toxicity to marine ecosystem. Low values of DOP and DOS indicate that pyritization and sulphidization are not being limited by the availability of reactive Fe. Sediment in these areas restricts the threat from sulfide to benthic organisms. An oil spill in part of the studied area has resulted in enhanced accumulation of AVS in marine sediment, resulting in a higher toxicity risk.

Acknowledgments

This work was financially supported by the National Natural Science Foundation of China (Grant No.: 41373100). Additional support was provided by Science and Technology Program for Public Wellbeing of Shandong Province (Grant No.:2013kjhm060308).

References

Bagarinao T., 1992. Sulfide as an environmental factor and toxicant: tolerance and adaptations in aquatic organisms, *Aquatic Toxicology* 24, 21-62.

Berner, R.A., 1970. Sedimentary pyrite formation. *American Journal of Science* 268, 1-23.

Berner, R.A., 1982. Burial of organic carbon and pyrite sulphur in the modern ocean: its geochemical and environmental significance. *American Journal of Science* 282, 451-473.

Berner, R.A., 1984. Sedimentary pyrite formation: an update. *Geochimica et Cosmochimica Acta* 48, 605-615.

Boesen, C., Postma, D., 1988. Pyrite formation in anoxic environments of the Baltic. *American Journal of Science* 288, 575-603.

Bottrell, S.H., Newton, R.J. 2006. Reconstruction of changes in global sulfur cycling from marine sulfate isotopes. *Earth-Science Reviews* 75, 59-83.

Bottrell S.H., Mortimer R.J.G, Davies I.M., Harvey S.M., Krom M.D., 2009. Sulphur cycling in organic-rich marine sediments from a Scottish fjord. *Sedimentology* 56, 1159-1173.

Burton, E.D., Bush, R.T., Johnston, S.G., Sullivan, L.A., Keene, A.F. 2011. Sulfur biogeochemical cycling and novel Fe-S mineralization pathways in a tidally re-flooded wetland. *Geochimica et Cosmochimica Acta* 75, 3434-3451.

Butler, I.B., Rickard, D. 2000. Framboidal pyrite formation via the oxidation of iron (II) monosulfide by hydrogen sulfide. *Geochimica et Cosmochimica Acta* 64, 2665-2672.

Canfield, D.E., Thamdrup, B., 1994. The production of ^{34}S-depleted sulfide during bacterial disproportionation of elemental sulfur. *Science* 266, 1973-1975.

Canfield, D.E., Raiswell, R., Bottrell, S., 1992. The reactivity of sedimentary iron minerals toward sulfide. *American Journal of Science* 292, 659-683.

Canfield, D.E., Kristensen, E., Thamdrup, B., 2005. The Sulfur Cycle, *Advances in Marine Biology* 48, 313-381.

Hsieh Y. P., Shieh Y. N., 1997. Analysis of reduced inorganic sulfur by diffusion

methods: improved apparatus and evaluation for sulfur isotopic studies. *Chemical Geology*, 137, 255-261.

Huerta-Dı′az, M.A., Morse, J.W., 1990. A quantitative method for determination of trace metal concentrations in sedimentary pyrite. *Marine Chemistry* 29, 119-144.

Hurtgen, M.T., Lyons, T.W., Ingall, E.D., Cruise, A.M. 1999. Anomalous enrichments of iron monosulfide in euxinic marine sediments and the role of H_2S in iron sulfide transformations: examples from Effingham Inlet, Orca basin, and the Black Sea. *American Journal of Science* 299, 556-588.

Kang, X., Liu, S. and Zhang, G. 2014. Reduced inorganic sulfur in the sediments of the Yellow Sea and East China Sea. Acta Oceanologica Sinica 33,100-108.

Lin, S., Huang, K.-M., Chen, S.-K., 2000. Organic carbon deposition and its control on iron sulfide formation of the southern East China Sea continental shelf sediments. *Continental Shelf Research* 20, 619-635.

Lin, S., Huang, K. M., Chen, S. K., 2002. Sulfate reduction and iron sulfide mineral formation in the southern East China Sea continental slope sediment. *Deep Sea Research Part I: Oceanographic Research Papers* 49, 1837-1852.

Liu H., Yin B., 2007. Annual cycle of carbon, nitrogen and Phosphorus in the Bohai Sea: A model study, *Continental Shelf Research* 27, 1399-1407.

Liu D., Keesing J.K, He P., Wang Z., Shi Y., Wang Y., 2013. The world's largest macroalgal bloom in the Yellow Sea, China: Formation and implications, *Estuarine, Coastal and Shelf Science* 129, 2-10.

Lv Y., Zhang W., Gao Y., Ning S., Yang B., 2011. Preliminary study on responses of

marine nematode community to crude oil contamination in intertidal zone of Bathing Beach, Dalian, *Marine Pollution Bulletin*, 62, 2700-2706.

Morgan, B., Burton, E.D., Rate, A.W., 2012. Iron monosulfide enrichment and the presence of organosulfur in eutrophic estuarine sediments, *Chemical Geology* 296-297, 119-130.

Morse, J.W., 1999. Sulfides in sandy sediments: new insights on the reactions responsible for sedimentary pyrite formation. *Aquatic Geochemistry* 5, 75-85.

Morse, J.W., Berner, R.A., 1995. What determines sedimentary C-S ratios. *Geochim. Cosmochim. Acta* 59, 1073-1077.

Morse, J.W., Rickard, D., 2004. Chemical dynamics of sedimentary acid volatile sulfide. *Environmental Science & Technology* 38, 131A-136A.

Morse, J.W., Thomson, H., Finneran, D.W., 2007. Factors controlling sulfide geochemistry in sub-tropical estuarine and bay sediments. *Aquatic Geochemistry* 13, 143-156.

Newton R. J., Bottrell S.H., Dean S.P., Hatfield D., Raiswell R., 1995. An evaluation of the use of the chromous chloride reduction method for isotopic analyses of pyrite in rocks and sediment, *Chemical Geology* 125, 317-320.

Phillips B. M., Anderson B. S., Hunt J. W., 1997. Measurement and distribution of interstitial and overlying water ammonia and hydrogen sulfide in sediment, *Marine Environmental Research* 44, 117-126.

Poulton, S.W. 2003. Sulfide oxidation and iron dissolution kinetics during the reaction of dissolved sulfide with ferrihydrite. *Chemical Geology* 202, 79-94.

Qiao S, Shi X, Zhu A, Liu Y., Bi N., Fang X., Yang G., 2010, Distribution and transport of suspended sediments off the Yellow River (Huanghe) mouth and the nearby Bohai Sea. *Estuarine, Coastal and Shelf Science* 86, 337–344.

Rickard, D., Morse, J.W., 2005. Acid volatile sulfide (AVS). *Marine Chemistry* 97, 141-197.

Rodrigues S.K., Abessa D.M.S., Machado E.C., 2013. Geochemical and ecotoxicological assessment for estuarine surface sediments from Southern Brazil, *Marine Environmental Research* 91, 68-79.

Rozan, T.F., Taillefert, M., Trouborst, R.E., Glazer, B.T., Ma, S. 2002. Iron-sulfur-phosphorous cycling in the sediments of a shallow coastal bay:implications for sediment nutrient release and benthic macro-algal blooms. *Limnology and Oceanography* 47, 1346-1354.

Schoonen, M.A.A., Barnes, H.L. 1991. Mechanisms of pyrite and marcasite formation from solution: III Hydrothermal processes. *Geochim. Cosmochim. Acta* 55, 3491-3504.

Sheng, Y., Fu, G.., Chen F., Chen J., 2011.Geochemical characteristics of inorganic sulfur in Shijing River, South China. *Journal of Environmental Monitoring* 13, 807 - 812.

Sheng, Y., Sun, Q., Bottrell, S.H., Mortimer, R.J.G., Shi, W., 2013. Anthropogenic impacts on reduced inorganic sulfur and heavy metals in coastal surface sediments, north Yellow Sea, *Environmental Earth Sciences* 68, 1367-1374.

Simpson, S.L., Ward, D., Strom, D., Jolley, D.F., 2012. Oxidation of acid-volatile

sulfide in surface sediments increases the release and toxicity of copper to the benthic amphipod Melita plumulosa, *Chemosphere* 88, 953-961.

Sorokin, Y.I., Zakuskina, O.Y., 2012. Acid-labile sulfides in shallow marine bottom sediments: A review of the impact on ecosystems in the Azov Sea, the NE Black Sea shelf and NW Adriatic lagoons, *Estuarine, Coastal and Shelf Science* 98, 42-48.

Tarpgaard, I.H., Røy, H., Jørgensen, B.B., 2011. Concurrent low- and high-affinity sulfate reduction kinetics in marine sediment, *Geochimica et Cosmochimica Acta*, 75, 2997-3010.

Xu, K., Milliman, J.D., Li, A., Liu, J.P., Kao, S.-J., Wan, S., 2009. Yangtze- and Taiwan-derived sediments on the inner shelf of East China Sea. Continental Shelf Research 29, 2240–2256.

Yin, H., Fan, C., Ding, S., Zhang, L. and Zhong, J., 2008. Geochemistry of Iron, Sulfur and Related Heavy Metals in Metal-Polluted Taihu Lake Sediments, *Pedosphere* 18, 564-573.

Zhou, J., Wu, Y., Kang, Q., Zhang, J., 2007. Spatial variations of carbon, nitrogen, phosphorous and sulfur in the salt marsh sediments of the Yangtze Estuary in China, *Estuarine, Coastal and Shelf Science* 71, 47-59.

Zhu, M., Liu, J., Yang, G., Li, T., Yang, R., 2012. Reactive iron and its buffering capacity towards dissolved sulfide in sediments of Jiaozhou Bay, China, *Marine Environmental Research* 80, 46-55.

Zhu, M., Shi X., Yang G., Hao X., 2013. Formation and burial of pyrite and organic

sulfur in mud sediments of the East China Sea inner shelf: Constraints from solid-phase sulfur speciation and stable sulfur isotope, *Continental Shelf Research* 54, 24-36.

Figure captions

Fig. 1 Location of studying areas and sampling sites

Fig. 2 Grain size distribution of surface sediments in different sampling sites

Fig. 3 Concentrations of TOC, TN and TS in surface sediment in different locations

Fig.4 Concentrations of different fractions of RIS in surface sediments (Note: sites B30, B31 and B32 were illustrated with the different scales)

Table 1 Calculation results of different measured geochemical parameters and different iron concentrations (μmol g^{-1}).

Yellow Sea	C/N	C/S	AVS/CRS	DOP	DOS	Fe_R	Fe_{py}	**Bohai Sea**	C/N	C/S	AVS/CRS	DOP	DOS	Fe_R	Fe_{py}
B01	7.84	6.67	0.08	0.04	0.04	147.43	5.70	B40	15.07	10.69	0.22	0.01	0.02	66.97	1.21
B02	11.92	14.70	0.23	0.03	0.05	113.41	3.85	B41	16.01	9.46	0.90	0.03	0.06	76.03	1.11
B03	17.22	11.81	0.94	0.02	0.07	65.53	1.12	B43	17.68	10.82	0.77	0.02	0.05	100.66	2.80
B04	16.43	13.29	0.12	0.01	0.01	110.69	0.77	B44	19.49	11.99	0.74	0.02	0.05	92.21	2.08
B05	16.09	17.28	0.17	0.03	0.04	71.51	2.04	B45	23.36	16.13	0.43	0.01	0.03	91.21	1.95
B07	12.99	8.74	0.07	0.04	0.05	85.19	3.72	B46	18.79	15.11	0.40	0.03	0.05	110.01	1.64
B09	10.00	11.28	0.09	0.03	0.04	65.35	2.17	B47	16.95	12.58	1.22	0.01	0.03	110.69	3.71
B13	12.52	3.50	0.05	0.09	0.10	46.95	4.39	B48	18.81	15.97	0.43	0.01	0.03	94.68	1.27
B15	8.34	1.31	0.15	0.02	0.03	22.56	0.39	B49	13.68	9.35	0.46	0.01	0.03	43.94	0.35
B21	9.71	5.35	0.14	0.03	0.05	50.42	1.73	B50	13.90	12.94	1.19	0.01	0.10	83.22	1.13
B23	11.58	5.45	0.06	0.04	0.05	63.96	3.00	B51	13.27	7.89	0.25	0.01	0.02	39.03	0.31
B24	10.40	6.81	0.16	0.03	0.04	100.27	3.19	B52	10.07	11.13	0.15	0.01	0.01	117.96	1.67
B25	9.60	9.07	0.08	0.06	0.07	84.73	5.43	B53	23.58	10.76	0.15	0.02	0.03	124.98	1.48
B26	18.50	11.33	0.53	0.01	0.03	69.19	1.03	B54	15.51	6.17	0.20	0.03	0.04	66.43	1.20
B28	24.53	18.66	0.33	0.01	0.02	56.19	0.43	B55	12.73	6.42	0.16	0.01	0.04	91.50	3.10
B30	8.16	2.60	0.01	0.27	0.28	77.35	28.79	B56	15.11	6.99	0.19	0.02	0.02	65.25	0.97
B31	41.32	12.47	0.02	0.31	0.33	39.32	17.74	B59	14.94	9.62	0.49	0.02	0.04	83.94	1.65
B32	15.81	4.82	0.04	0.28	0.32	76.56	30.24	B60	14.90	12.83	0.14	0.04	0.04	78.57	1.65
B33	20.87	10.37	0.19	0.03	0.07	28.29	0.98	B61	11.97	6.64	0.26	0.03	0.04	113.02	4.93
B34	16.08	9.35	0.40	0.01	0.02	40.57	0.54	B62	10.48	10.93	0.16	0.02	0.03	138.62	3.62
B37	14.10	12.85	0.28	0.02	0.05	53.68	1.13	B63	13.32	10.62	0.18	0.02	0.02	124.58	1.91
B38	15.29	13.56	0.39	0.02	0.03	70.55	1.29	B64	18.40	12.39	0.77	0.02	0.03	114.49	2.04
H01	24.94	24.28	0.64	0.01	0.01	102.20	0.79	B66	29.69	37.48	0.83	0.03	0.05	71.33	1.19
H02	22.77	24.22	0.16	0.01	0.01	74.91	0.62	B67	27.41	13.18	0.14	0.01	0.02	88.67	2.65

H03	19.12	15.18	0.42	0.00	0.01	71.08	0.17	B68	34.54	12.45	0.20	0.02	0.02	66.03	0.69
H04	11.89	9.41	0.51	0.01	0.02	110.87	1.55	B69	20.17	12.28	0.93	0.02	0.02	94.15	1.71
H05	8.87	7.28	0.06	0.02	0.03	165.16	4.22	B70	21.00	15.01	1.20	0.04	0.04	91.89	1.60
H06	8.32	6.14	1.09	0.02	0.03	163.58	3.16	YD1	48.41	30.10	0.36	0.01	0.02	77.82	0.68
H07	7.71	6.92	0.05	0.02	0.02	172.32	3.55	Mean	18.90	12.78	0.48	0.02	0.04	89.92	1.80
H08	8.35	7.45	0.18	0.02	0.03	185.00	3.82	**East China Sea**							
H09	8.25	6.32	0.08	0.04	0.04	159.28	6.35	H42	16.81	6.52	0.08	0.04	0.05	127.45	5.76
H10	8.57	11.20	0.10	0.03	0.03	150.15	4.57	E01	16.73	13.32	0.11	0.03	0.04	171.85	4.92
H11	9.58	5.87	0.02	0.04	0.04	179.19	7.25	E02	18.69	16.97	0.09	0.04	0.05	111.37	4.74
H12	9.69	7.40	0.12	0.02	0.03	164.26	3.24	E03	17.96	6.50	0.04	0.03	0.03	148.40	4.47
H14	10.80	10.14	0.46	0.01	0.03	91.82	1.04	E04	20.75	8.45	0.03	0.03	0.03	110.37	3.67
H16	16.18	7.27	0.96	0.01	0.02	52.46	0.59	E05	15.64	10.20	0.04	0.04	0.04	111.37	4.76
H43	9.26	9.02	0.11	0.03	0.04	181.77	5.49	Mean	17.76	10.33	0.07	0.04	0.04	130.14	4.72
H44	9.10	10.15	0.15	0.02	0.03	178.48	4.47								
HF1	12.48	11.32	0.13	0.01	0.02	50.35	0.54								
HF3	8.34	8.38	0.05	0.03	0.04	138.33	4.48								
H29	12.53	12.26	0.08	0.02	0.03	140.30	3.29								
H31	14.47	7.65	0.18	0.03	0.04	134.50	3.53								
H32	17.42	13.03	0.08	0.02	0.03	147.61	3.20								
H33	24.68	8.46	0.07	0.02	0.04	108.76	2.76								
H34	20.65	8.10	0.07	0.03	0.03	140.27	3.69								
H35	40.87	21.72	0.07	0.02	0.02	105.43	1.64								
H36	33.38	16.84	0.17	0.02	0.03	98.98	2.00								
H38	20.68	13.88	0.08	0.02	0.02	139.05	2.91								
Mean	15.17	10.44	0.22	0.04	0.05	103.04	4.14								

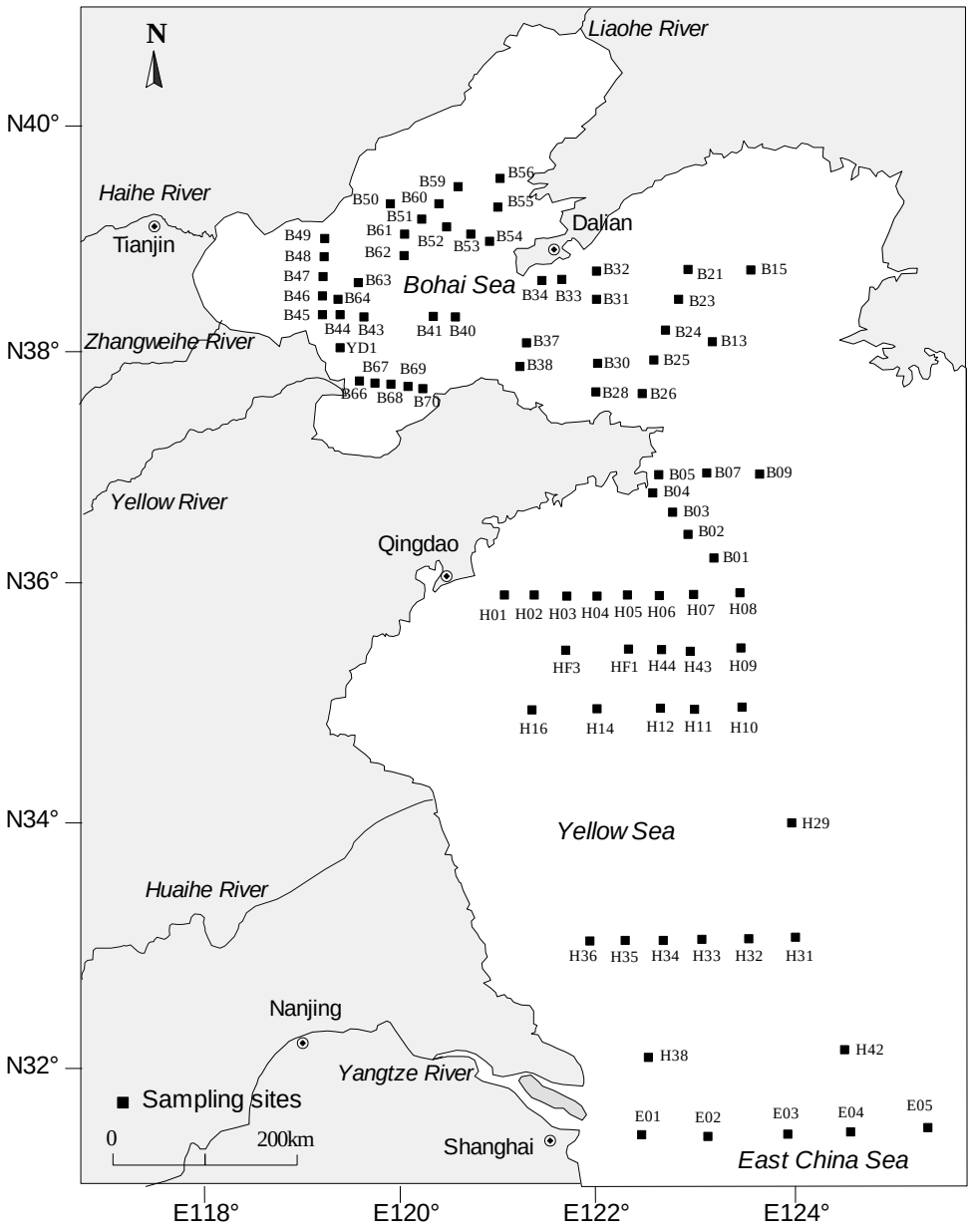
N
Liaohe River
Haihe River
Tianjin
Dalian
Bohai Sea
Zhangweihe River
Yellow River
Qingdao
Yellow Sea
Huaihe River
Nanjing
Yangtze River
Shanghai
East China Sea
Sampling sites
0
200km
N40°
N38°
N36°
N34°
N32°
E118°
E120°
E122°
E124°
B59 B56 B50 B60 B55 B51 B61 B52 B53 B54 B49 B62 B48 B47 B63 B46 B64 B45 B44 B43 B41 B40 YD1 B67 B69 B66 B68 B70 B32 B21 B15 B34 B33 B31 B23 B37 B24 B13 B38 B30 B25 B28 B26 B05 B07 B09 B04 B03 B02 B01 H01 H02 H03 H04 H05 H06 H07 H08 HF3 HF1 H44 H43 H09 H16 H14 H12 H11 H10 H29 H36 H35 H34 H33 H32 H31 H38 H42 E01 E02 E03 E04 E05

Fig. 1

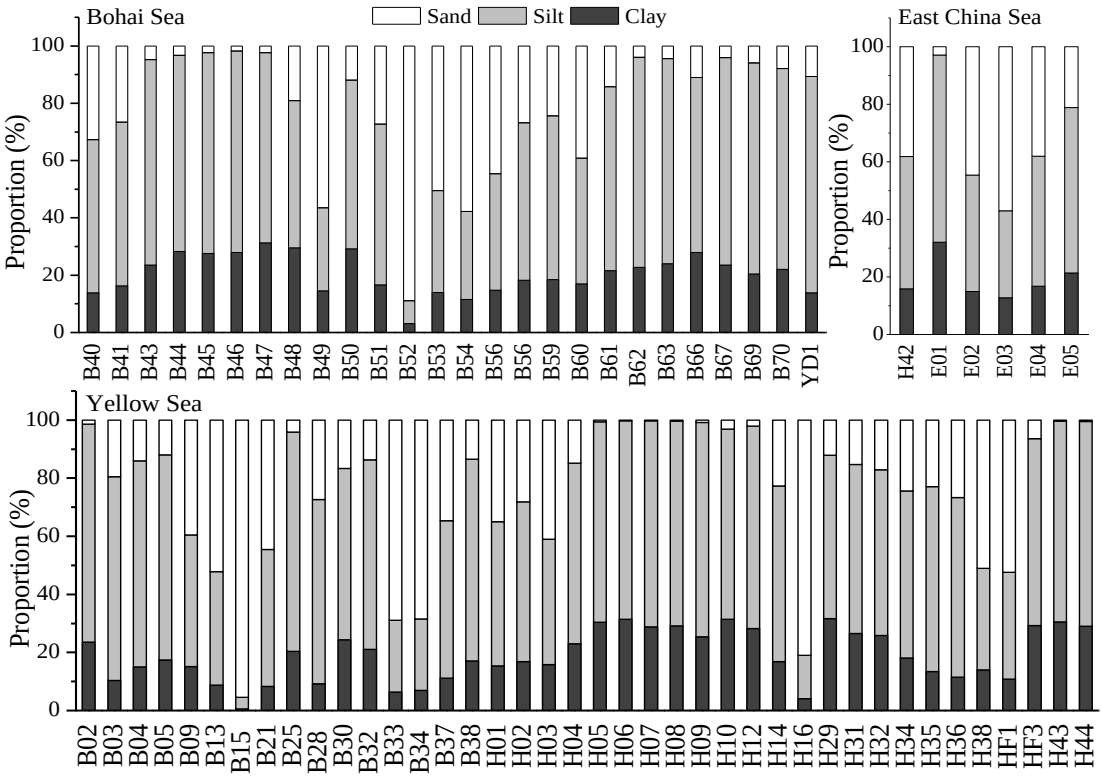
Bohai Sea
Sand
Silt
Clay
East China Sea
Yellow Sea
Proportion (%)
0
20
40
60
80
100
B40
B41
B43
B44
B45
B46
B47
B48
B49
B50
B51
B52
B53
B54
B56
B56
B59
B60
B61
B62
B63
B66
B67
B69
B70
YD1
H42
E01
E02
E03
E04
E05
B02
B03
B04
B05
B09
B13
B15
B21
B25
B28
B30
B32
B33
B34
B37
B38
H01
H02
H03
H04
H05
H06
H07
H08
H09
H10
H12
H14
H16
H29
H31
H32
H34
H35
H36
H38
HF1
HF3
H43
H44

Fig. 2

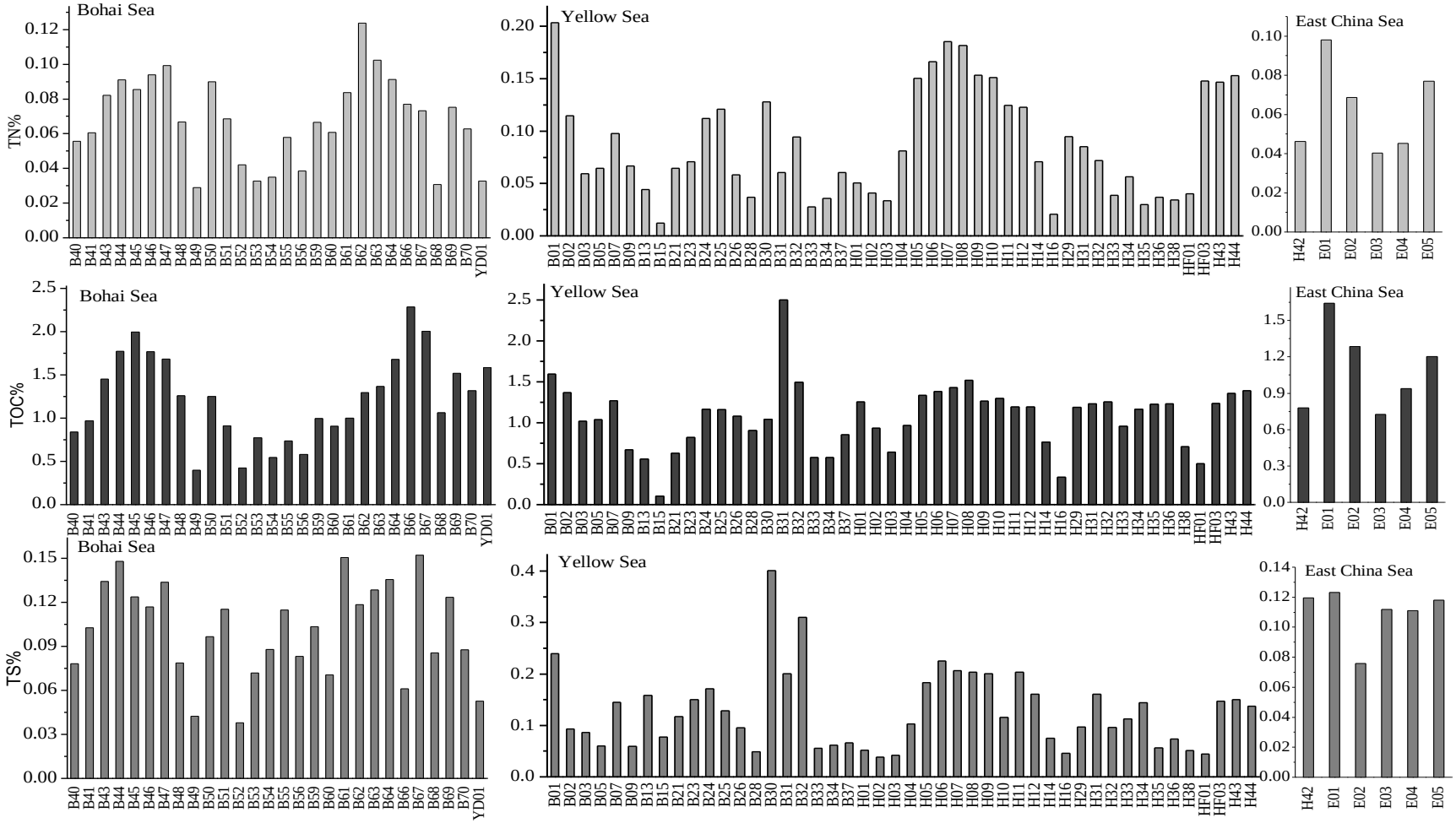
Bohai Sea
Yellow Sea
East China Sea
TN%
TOC%
TS%
B40 B41 B43 B44 B45 B46 B47 B48 B49 B50 B51 B52 B53 B54 B55 B56 B59 B60 B61 B62 B63 B64 B66 B67 B68 B69 B70 YD01
B01 B02 B03 B05 B07 B09 B13 B15 B21 B23 B24 B25 B26 B28 B30 B31 B32 B33 B34 B37 H01 H02 H03 H04 H05 H06 H07 H08 H09 H10 H11 H12 H14 H16 H29 H31 H32 H33 H34 H35 H36 H38 HF01 HF03 H43 H44
H42 E01 E02 E03 E04 E05

Fig. 3

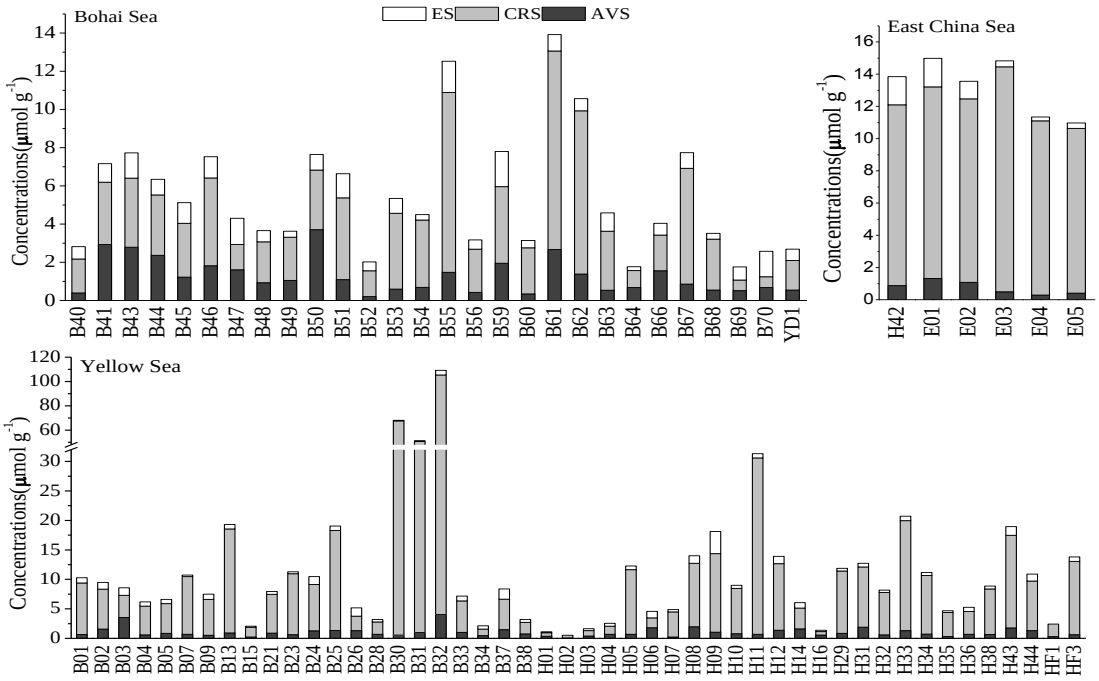
Bohai Sea
ES
CRS
AVS
East China Sea
Yellow Sea
Concentrations(μmol g-1)
B40 B41 B43 B44 B45 B46 B47 B48 B49 B50 B51 B52 B53 B54 B55 B56 B59 B60 B61 B62 B63 B64 B66 B67 B68 B69 B70 YD1
H42 E01 E02 E03 E04 E05
B01 B02 B03 B04 B05 B07 B09 B13 B15 B21 B23 B24 B25 B26 B28 B30 B31 B32 B33 B34 B37 B38 H01 H02 H03 H04 H05 H06 H07 H08 H09 H10 H11 H12 H14 H16 H29 H31 H32 H33 H34 H35 H36 H38 H43 H44 HF1 HF3

Fig.4